

# Optimized population Monte Carlo

P. L. Ebert<sup>1</sup>, D. Gessert<sup>2,3</sup>, W. Janke<sup>2</sup>, and M. Weigel<sup>1,\*</sup>

<sup>1</sup> Institut für Physik, Technische Universität Chemnitz, 09107 Chemnitz, Germany,

<sup>2</sup> Institut für Theoretische Physik, Leipzig University, IPF 231101, 04081 Leipzig, Germany

<sup>3</sup> Centre for Fluid and Complex Systems, Coventry University, Coventry CV1 5FB, United Kingdom

**Abstract.** Population Monte Carlo simulations in the form commonly referred to as population annealing can serve as a useful meta-algorithm for simulating systems with complex free-energy landscapes. In the present paper we provide an easily accessible introduction to the approach, focusing on spin systems as simple example problems. While the method is very general and powerful, it also comes with a number of tunable parameters. Here, we discuss the question of an optimal choice of resampling protocol, that is shown to have significant influence on the quality of results. While population annealing is an excellent fit to the paradigm of massively parallel simulations, limitations in the availability of parallel resources and especially memory can provide a bottleneck to its efficacy. As we demonstrate for results of the Ising ferromagnetic and spin-glass models, weighted averages of smaller-scale runs can be easily combined to reduce both systematic and statistical errors in order to avoid such bottlenecks.

## 1 Introduction

Population annealing was first introduced by Hukushima and Iba in Ref. [1] based on some earlier more general proposals [2]. In statistical physics, however, it received little attention before a later rediscovery by Machta [3]. In this framework, an equilibrated population of system copies is considered at a fixed temperature. The temperature is then lowered in small steps, such that the population undergoes annealing towards a target temperature. In each step, each copy (replica) experiences a weight modification that depends on its own likelihood in the ensemble at the lower temperature [4]. Population control is then used to ensure that only sufficiently important configurations are further followed through the cooling process.

In this way, population annealing combines several strategies to work towards good sampling of systems with metastability and energetic or entropic barriers: through the presence of a (large) population, metastable minima can be occupied according to their relative free-energy weight without ever having to cross any intervening barriers; population control accelerates equilibration and

---

\* Email: martin.weigel@physik.tu-chemnitz.de

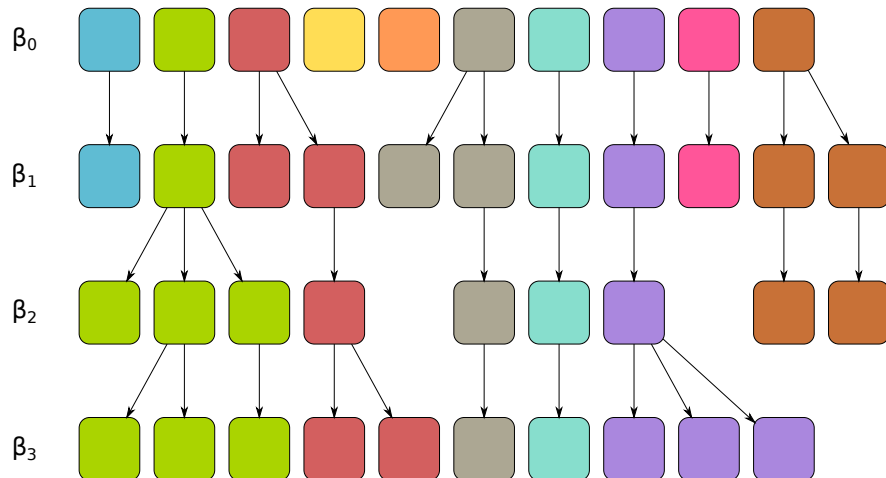


**Fig. 1.** Illustration of the population in PA, propagated from the initial inverse temperature  $\beta_0$  to a higher inverse temperature  $\beta_3$ . At each temperature step, the resampling replicates some configurations while eliminating others. Members of the same *family* (descendants from the same configuration in the initial population at  $\beta_0$ ) are shown in the same color.

ensures importance sampling of different valleys; finally, a free choice of algorithms for regular update steps taken at fixed temperature allows to efficiently keep the population equilibrated through the anneal [4]. This last possibility to combine the scheme with many different “driver algorithms”, including cluster updates or even molecular dynamics simulations [5], as well as the freedom of choice regarding the annealing parameters and probability weights [6–8], turns the framework into a rather versatile meta-algorithm for computer simulations.

The main strength of the approach over related schemes such as parallel tempering or replica exchange simulations [9–11] might lie in its outstanding parallel performance, however. For practical applications, population sizes of  $10^3 - 10^6$  replicas are usually required, providing very direct opportunities to use a number of processing units that is of the same order of magnitude [12]. Parallel tempering, on the other hand, is usually not very efficient for more than 100 replicas. This renders population annealing the tool of choice for computer simulations in the era of massively parallel computing [13].

## 2 The algorithm

In its original formulation, population annealing (PA) starts with an ensemble of equilibrium samples at inverse temperature  $\beta_0$  that is then sequentially cooled until it reaches the final temperature  $\beta_f$ . The target distribution here corresponds to the Gibbs-Boltzmann form  $\pi_\beta = Z_\beta^{-1} \exp(-\beta E)$ , where  $Z_\beta$  denotes the partition function and  $E$  is the internal energy of the system. In the process,

a combination of single-replica update steps — usually realized through Markov chain Monte Carlo (MCMC) — and resampling of the population is employed to ensure that the population remains well equilibrated. The process is illustrated in Fig. 1. The individual steps of the approach can be summarized as follows:

1. Initialize  $R_0 = R$  replicas with configurations drawn from  $\pi_{\beta_0}$ . For  $\beta_0 = 0$ , this is usually possible via exact sampling, otherwise an approximation (equilibration) is required, for example using MCMC.
2. Resample the population from the current inverse temperature  $\beta_{i-1}$  to  $\beta_i > \beta_{i-1}$ , replicating configurations according to their relative weight at  $\beta_i$ ,

$$\tau_i(E_j) = \exp[-(\beta_i - \beta_{i-1})E_j]/Q_i,$$

where  $\beta_i - \beta_{i-1} = \Delta\beta_i$  and

$$Q_i \equiv Q(\beta_{i-1}, \beta_i) = \frac{1}{R_{i-1}} \sum_{j=1}^{R_{i-1}} \exp[-(\beta_i - \beta_{i-1})E_j]. \quad (1)$$

3. To improve equilibration at  $\beta_i$ , subject each replica to  $\theta_i$  rounds of single-replica updates (e.g., MCMC).
4. Take measurements of any observable  $\mathcal{O}$  as a population average,  $\sum_{j=1}^{R_i} \mathcal{O}_j/R_i$ , where  $R_i$  is the population size at the  $i$ th temperature step.
5. Return to step 2 unless the target temperature  $\beta_f$  has been reached.

For systems without hard constraints, equilibrium configurations at  $\beta_0 = 0$  can easily be generated using simple sampling. For  $\beta_0$  positive but small, equilibration with MCMC is easily possible. In the presence of constraints, it can be useful to choose a set of independent coordinates. The stepwise cooling of the population that lends PA its name results in the replicas acquiring individual weights that depend on the internal energy  $E_j$ . In particular, at each step  $\beta_{i-1} \rightarrow \beta_i$  each replica acquires an incremental importance weight

$$\gamma_i^j = \frac{Z_{\beta_{i-1}}}{Z_{\beta_i}} e^{-(\beta_i - \beta_{i-1})E_j^{i-1}},$$

such that at the  $i$ th step the total weight becomes  $W_i^j = W_{i-1}^j \gamma_i^j$ . In the version of the algorithm outlined above, however, the resampling procedure at each temperature step results in a replication of each configuration proportional to  $\gamma_i^j$ . As a consequence, the weights  $W_i^j$  do not need to be considered and the observable estimates in step 4 can be computed as plain, unweighted averages. Different suitable realizations of the resampling process and their properties are discussed in Sec. 3.

After resampling, the weight of each surviving copy needs to be modified by a factor of  $1/\tau_i(E_j)$ , resulting in a renormalized weight of

$$\begin{aligned} \widetilde{W}_i^j &= \widetilde{W}_{i-1}^j \frac{\gamma_i^j}{\tau_i(E_j)} = \widetilde{W}_{i-1}^j \frac{Z_{\beta_{i-1}}}{Z_{\beta_i}} Q_i \\ &= W_0^j \frac{Z_0}{Z_{\beta_1}} \dots \frac{Z_{\beta_{i-1}}}{Z_{\beta_i}} \prod_{k=1}^i Q_k = \frac{1}{Z_{\beta_i}} \prod_{k=1}^i Q_k. \end{aligned} \quad (2)$$

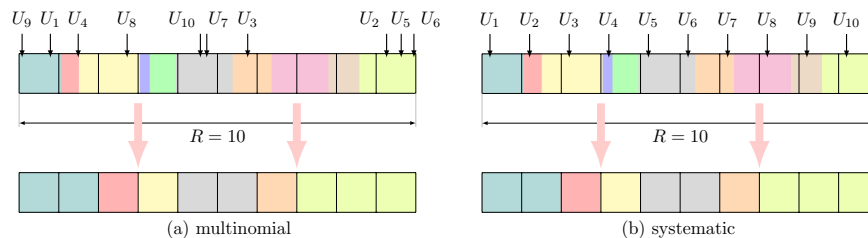


**Fig. 2.** Two resampling methods for constant population size: (a) multinomial resampling and (b) systematic resampling. The colored boxes represent the size of the resampling factors  $\tau_i^j$  and members of the resampled population are chosen according to the color at the position of the labels  $U_1, \dots, U_R$ .

Clearly, these weights are independent of  $j$ , but they depend on the normalization factors  $Q_k$  that are random variables with respect to different population annealing simulations using the same parameters  $R, \theta, \Delta\beta$  etc. As a consequence, if such simulations are repeated to improve results, their combination requires *weighted* averaging in order to reduce both, systematic and statistical errors. This aspect is discussed below in Sec. 4.

In total, the uni-directional stepping through successive temperatures sets the approach apart from the MCMC paradigm and it is, in fact, a sequential Monte Carlo algorithm [14]. In combination with the MCMC component that is usually used as the equilibrating subroutine in step 3, the properties of PA combine elements of MCMC and sequential MC which somewhat complicates its systematic analysis. A comprehensive discussion of its properties in this respect was given in Refs. [4, 15].

### 3 Resampling methods

The resampling step in PA comes with considerable freedoms. While it is crucial for ensuring that the most important areas of configuration space are sampled instead of wasting substantial effort on configurations contributing negligible weight to the final averages, it is not strictly necessary to resample in every temperature step. In some cases it might be sufficient to execute population control once the variance of importance weights becomes too large [16]. More fundamentally, the goal of achieving equal weight of all resulting population members only requires that the *expected* number of copies follows the weights, i.e., if  $r_i^j$  copies are made of replica  $j$  in temperature step  $i$ , then we require that

$$\langle r_i^j \rangle = \tau_i^j.$$

The actual probability distribution of  $r_i^j$  is not constrained by the algorithm and hence a tunable dimension. A fundamental distinction arises between approaches where the population size remains constant in each step, i.e.,  $R_i = R_{i-1} = R$ , and schemes with fluctuating population size.

For *fixed population size*, the physics literature has so far focused on the *multinomial* distribution [1], and only recently have other approaches been considered [17, 18]. One particularly simple alternative is *systematic* resampling. These two techniques are illustrated in Fig. 2, where the replication weights  $\tau_i^j$  are represented by adjacent colored boxes, whose total width adds up to  $R$ . Resampling with fixed population size then amounts to drawing  $R$  new replicas with probabilities proportional to  $\tau_i^j$ . For the multinomial approach shown in Fig. 2(a),  $R$  random numbers  $U_i$  are uniformly drawn from the interval  $[0, R]$ , each creating a replica corresponding to the color at the marked location. In contrast, in systematic resampling, only a single uniform random number  $U_1 \in [0, 1]$  is drawn while the remaining labels are placed at  $U_k = U_{k-1} + 1$ ,  $k = 2, \dots, R$ , cf. Fig. 2(b).

For *variable population size*, on the other hand, popular techniques include *Poisson* resampling [3] as well as the *nearest-integer* method, where  $\lfloor \tau_i^j \rfloor$  copies<sup>5</sup> are made for each replica of the original population and an additional copy with probability  $\tau_i^j - \lfloor \tau_i^j \rfloor$  [15]. In order to suppress the occurrence of large fluctuations in the resulting population sizes  $R_i$ , rescaled resampling factors

$$\hat{\tau}_i^j = (R/R_{i-1})\tau_i^j \quad (3)$$

are usually used for methods with fluctuating population size. In order to simplify notation, we refer to all such factors as  $\tau_i^j$  where it is understood that for fluctuating population size  $\hat{\tau}_i^j$  should be used. The resulting fluctuations in  $R_i$  are of the order of  $\sqrt{R}$  and hence very moderate for practically used target population sizes.

In a test performing population annealing simulations for the Ising model on a  $L \times L$  square lattice with Hamiltonian

$$\mathcal{H} = -J \sum_{\langle ij \rangle} \sigma_i \sigma_j, \quad (4)$$

one finds moderate differences in the overall bias and statistical error between the different resampling schemes, cf. Fig. 3 [17, 18]. These are most pronounced in the vicinity of the ordering transition at  $\beta_c \approx 0.44068$ , with nearest-integer and systematic resampling resulting in the smallest and Poisson and multinomial resampling in the largest errors. These observations can be understood when considering the *sampling variance*,

$$\text{SV} = \frac{1}{R_i} \sum_{j=1}^{R_i} (\tau_i^j - \tau_i^j)^2, \quad (5)$$

which captures the additional noise introduced through the resampling process. As is seen from the estimates of SV shown in Fig. 4(a), better resampling methods have smaller sampling variance.

<sup>5</sup> Here,  $\lfloor \cdot \rfloor$  denotes the largest integer smaller than the argument, i.e., rounding down.

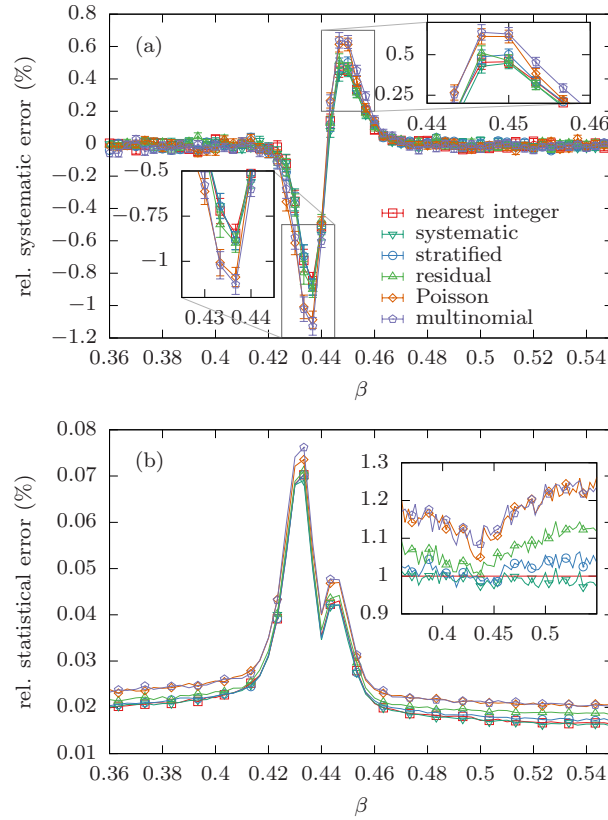


**Fig. 3.** Relative systematic (a) and statistical (b) error of the specific heat of the 2D Ising model for an  $L = 64$  system in PA simulations employing different resampling methods. The simulation parameters were  $R = 20\,000$ ,  $\theta = 5$ , and  $\beta_i = i/300$ .

For the specific case of the 2D Ising model, it is possible through the availability of exact results for the density of states to extrapolate these findings to perfectly equilibrated simulations with  $\theta \rightarrow \infty$  and infinite population sizes,  $R \rightarrow \infty$  [18], and the general trends of Figs. 3 and 4(a) remain unchanged in these limits. The interaction of resampling scheme and temperature protocol is more intricate: it is well known that too large steps result in extreme fluctuations [4], but we find that also too small steps lead to a systematic injection of additional noise for resampling schemes with larger sampling variances. This is illustrated in Fig. 4(b), which shows the *resampling cost*, i.e., the increase in the replica-averaged family size

$$\rho_t = R \sum_{k=1}^R n_k^2, \quad (6)$$

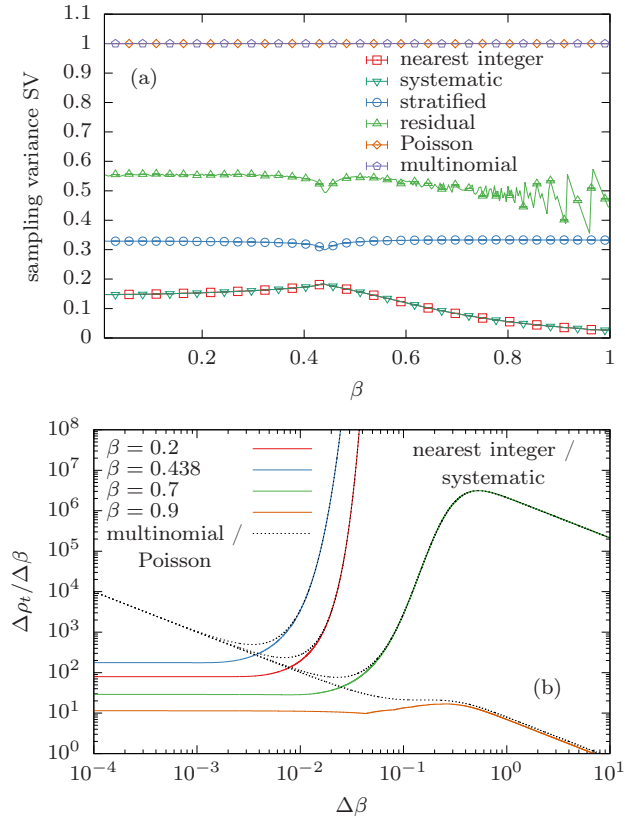


**Fig. 4.** (a) Sampling variance according to Eq. (5) for PA simulations of a  $64 \times 64$  2D Ising model using different resampling schemes shown as a function of inverse temperature  $\beta$  (simulations with  $R = 20\,000$ ,  $\theta = 5$ ,  $\beta_i = i/300$ ). (b) Resampling cost  $\Delta\rho_t/\Delta\beta$  as a function of inverse temperature step  $\Delta\beta$  for PA simulations of the 2D Ising model and nearest-integer/systematic resampling as compared to multinomial resampling ( $L = 64$ ,  $\theta = \infty$ ,  $R = \infty$ ).

per inverse temperature step,  $\Delta\rho_t/\Delta\beta$ . Here,  $\mathbf{n}_k$  denotes the fraction of the population that descends from replica  $k$  of the initial population. The quantity  $\rho_t$  is a measure for the degree of correlation introduced into the population through resampling [15] (see Ref. [4] for the alternative quantity  $R_{\text{eff}}$ ). It ranges from  $\rho_t = 1$  for an uncorrelated population to  $\rho_t = R$  for the case of only a single surviving family. While for multinomial resampling (as well as for other techniques discussed in Ref. [18]), the resampling cost increases without bound for (too) small temperature steps, it becomes independent of (sufficiently small) step size for nearest-integer and systematic resampling, cf. Fig. 4(b). This suggests that for these methods the choice of temperature step is less crucial, such that they

not only provide the least systematic and statistical error, but they are also more robust than alternative approaches.

## 4 Weighted averages

While population annealing is particularly well suited for highly parallel simulations [12,13], in some cases the desired population size might be hard to achieve due to limitations in the available memory. In other cases, one might be interested in reducing bias and statistical error of simulation results by performing additional PA runs. To achieve this, some averaging or data-pooling procedure is required. According to the discussion in Sec. 2 above, the necessary weights are related to the normalizing factors  $Q_k$  of Eq. (1). As can be readily shown, these encode a free-energy estimate according to [3]

$$-\beta_i \widehat{F}_i = \ln Z_{\beta_0} + \sum_{k=1}^i \ln Q_k. \quad (7)$$

Hence the weights of Eq. (2) become

$$\widetilde{W}_i^j = \frac{1}{Z_{\beta_i}} \prod_{k=1}^i Q_k = \frac{1}{Z_0 Z_{\beta_i}} \exp(-\beta_i \widehat{F}_i). \quad (8)$$

Consequently, the individual estimates  $\widehat{\mathcal{O}}_i^{(m)} \equiv \widehat{\mathcal{O}}^{(m)}(\beta_i)$ ,  $m = 1, \dots, M$ , from  $M$  different PA simulations at constant population size should be combined in a weighted fashion as

$$\mathcal{W}[\widehat{\mathcal{O}}_i] = \sum_{m=1}^M \omega_i^{(m)} \widehat{\mathcal{O}}_i^{(m)}, \quad (9)$$

with

$$\omega_i^{(m)} = \frac{R_i^{(m)} \exp(-\beta_i \widehat{F}_i^{(m)})}{\sum_m R_i^{(m)} \exp(-\beta_i \widehat{F}_i^{(m)})}. \quad (10)$$

For fluctuating population size the expressions become a bit more complicated, but the numerical differences are small [4,19].

While this prescription applies to plain averages of single-replica observables or *configurational estimators*, different strategies are required for more general quantities. One common class of such observables are central moments and, in particular, variances such as the specific heat and susceptibility. In such cases, one must apply the weighting to the (non-central) moments, resulting in the expressions [19]

$$\mathcal{W}_{\text{var}}[\widehat{c}] := \beta^2 N \left[ \mathcal{W}[\widehat{e}^2] - \left( \mathcal{W}[\widehat{e}] \right)^2 \right] \quad (11)$$

for the specific heat and

$$\mathcal{W}_{\text{var}}[\widehat{\chi}] := \beta N \left[ \mathcal{W}[\widehat{m}^2] - \left( \mathcal{W}[\widehat{m}] \right)^2 \right] \quad (12)$$



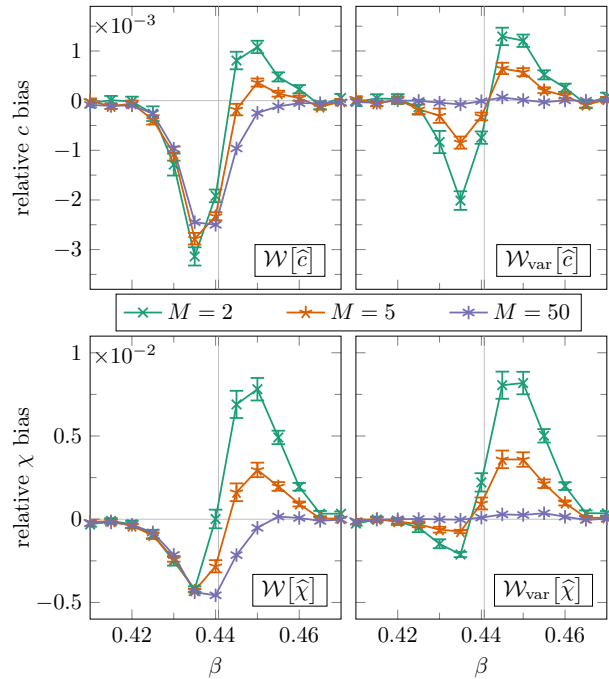


**Fig. 5.** Biases observed in weighted averages for the specific heat  $c$  per spin and the magnetic susceptibility per spin  $\chi$  for  $M$  PA simulations of the 2D Ising model with  $L = 64$ ,  $\theta = 10$  and  $R = 20\,000$  as a function of inverse temperature  $\beta$ . The location of the critical temperature is marked by the vertical lines. The results from the naive weighting scheme shown in the left column exhibit a merely moderate bias reduction, while for the corrected scheme of Eqs. (11) and (12) the bias quickly decays to zero as  $M$  is increased.

for the susceptibility, where  $\hat{e}$  and  $\hat{e}^2$  as well as  $\hat{m}$  and  $\hat{m}^2$  are the standard estimators (averages) of the first and second moments of the energy and magnetization, respectively. More general cases can be treated along similar lines [19].

Using these modified expressions, one finds that the biases of the weighted estimators of quantities such as the specific heat and susceptibility also systematically decrease as the number  $M$  of PA runs is increased. This is illustrated in Fig. 5 which shows the results of the naive weighting scheme on the left and those of the correct approach according to Eqs. (11) and (12) on the right. As is clearly visible, only the corrected scheme leads to a systematic bias reduction with increasing  $M$ . As is discussed in Ref. [19], this reduction in general follows a power law  $M^{-b}$  with  $0 \leq b \leq 1$  and  $b$  approaching 1 when the individual runs to be averaged over are very well equilibrated. More fundamentally, it can also be shown rigorously, that the empirical distribution represented by the weighted combination of individual runs converges to the equilibrium distribution as  $M \rightarrow \infty$  [19].

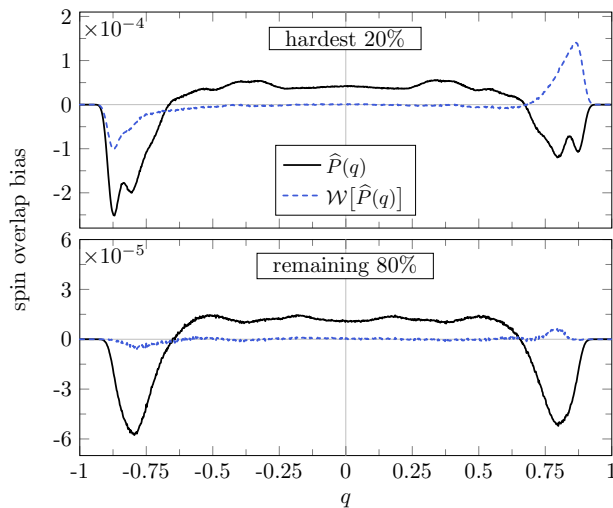


**Fig. 6.** Bias in the estimate  $\hat{P}(q)$  of the overlap distribution of the 2D bimodal Edwards-Anderson spin-glass model on the  $32 \times 32$  square lattice with periodic boundaries using 50 disorder samples. The PA runs used  $\theta = 25$  and  $R = 5 \times 10^6$  with 100 inverse temperature steps between  $\beta_0 = 0$  and  $\beta_f = 3$ . Here, the hardness of samples was judged according to the observed values of  $\rho_t$  at  $\beta_f$ .

The strength and limitations of the approach can be more accurately judged for problems such as spin glasses, where systematic errors due to incomplete equilibration are commonplace. In Fig. 6 we show the bias in the estimate of the overlap distribution  $\hat{P}(q)$  of the 2D Edwards-Anderson Ising spin-glass model with bimodal couplings: while for the bulk of the disorder samples a weighted average of the estimates from  $M = 50$  runs is able to all but eliminate bias at the level of the resolution of the simulation, for the hardest samples this reduction is noticeably weaker.

In an ideal world, the weighted combination of  $M$  PA simulations with populations of size  $R$  would be equivalent to a single simulation with population size  $MR$ . In reality, this can only be the case if there are no fluctuations that lead to correlations between more than  $\sim R$  replicas, since these could not be represented in the  $M$  simulations of size  $R$  each. As we illustrate in Fig. 7 with the overlap distribution of the 2D Edwards-Anderson model, bias is practically absent in the easiest disorder realization both in the weighted average of  $M$  simulations as well as in the big simulation of size  $MR$ . For the hardest instance considered, on the other hand, the larger simulation is significantly better than the weighted average of the smaller ones. Note that for the sake of illustration, the simulation parameters (in particular, the population size  $R = 2 \times 10^4$ ) were deliberately chosen such that the individual simulations are often not able to equilibrate some of the disorder samples.

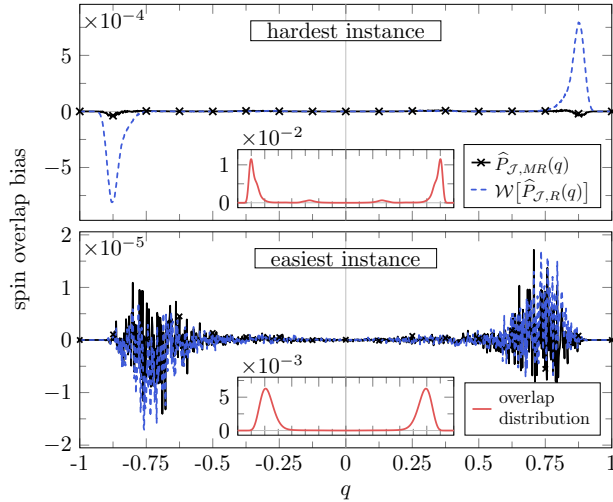


**Fig. 7.** Bias in estimating the overlap distribution of the 2D Ising spin glass for  $L = 32$ , comparing the weighted average of  $M = 50$  simulations with  $R = 20\,000$  to a single run of size  $MR = 10^6$ . For the easiest instance (according to  $\rho_t$  at  $\beta_f = 3$ ), there is no visible difference between these two strategies (bottom panel), while for the hardest instance the large simulation is significantly more efficient in reducing systematic error (top panel). The insets show the actual overlap distribution functions for the samples in question, illustrating the richer structure for the harder sample.

While the above considerations have focused on systematic errors, it is clear that weighted averaging also has an effect on statistical errors. In the case of very even simulation weights  $\omega_i^{(m)}$ , statistical errors are reduced by a factor  $\sim 1/\sqrt{M}$ . In the opposite extreme, a single simulation dominates in weight and hence a weighted average offers no reduction of statistical errors at all compared to a single run. Reductions of systematic and statistical errors are thus to a certain degree competing targets, and it is consequently of interest to consider a combined accuracy measure such as the root-mean-square deviation (RMSD), i.e.,

$$\text{RMSD} := \sqrt{\text{bias}^2 + \text{variance}}. \quad (13)$$

The behavior of the RMSD for weighted averages in PA simulations of the 2D Ising model is illustrated in Fig. 8, showing results for the internal energy and specific heat. Here, we deliberately choose a (too) small  $\theta = 2$  for the  $L = 64$  system in order to generate an appreciable systematic error. For the internal energy shown in the upper panel, plain averaging over up to  $M = 50$  simulations essentially has no effect on the RMSD in the critical regime, since there it is dominated by bias. In contrast, weighted averaging leads to a systematic decay of the deviation. For the specific heat, on the other hand, some decrease of the RMSD near the peak is visible also for plain averaging as the statistical error is more important there. Note, however, that due to the incremental nature of the

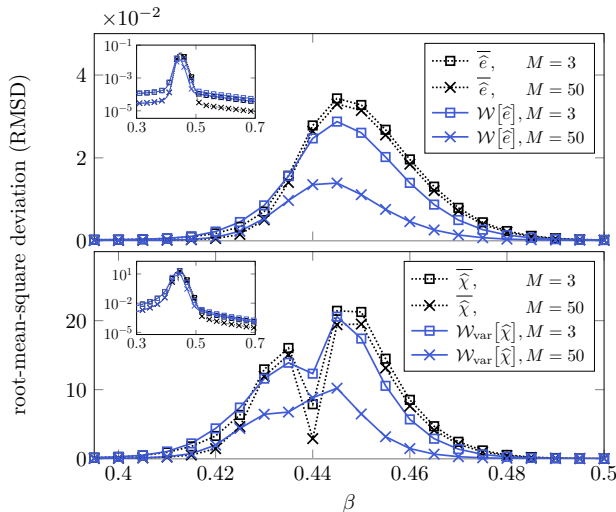


**Fig. 8.** Root-mean-squared deviation (RMSD) of estimates of the internal energy (top panel) and magnetic susceptibility (bottom panel) of the 2D Ising model from (quasi)exact reference data. The estimates are computed from  $M$  repeated PA simulations with  $L = 64$ ,  $\theta = 2$  and  $R = 20\,000$  using plain and weighted averages, respectively. The insets show the same data on a logarithmic scale.

free-energy estimators  $\hat{F}_i$  of Eq. (7) that enter the weights (10), uneven weights between runs triggered by systematic deviations near the critical point are also retained in the ordered phase, such that the weighted averages do not result in a significant reduction of statistical errors there.

Overall, if applied correctly, weighted averaging yields a powerful tool for the reduction of systematic errors while also, in most cases, reducing statistical errors by increasing the amount of data included. In many cases of at most moderate biases, such a weighted combination of repeated runs is even competitive with the naturally superior benchmark of a single run with a correspondingly larger population.

## 5 Conclusion and outlook

Population annealing is a promising and rather general meta-algorithm for computer simulations especially of systems with complex free-energy landscapes [20] that excels, in particular, through its near perfect fit to the massively parallel architectures of the high-performance computing landscape of exascale capabilities and beyond [12]. It can be combined with nearly arbitrary driver algorithms and is also portable to different annealing parameters such as energies in microcanonical simulations [7] or transverse fields in a quantum version [21]. In the present article we have given an introduction and overview for the approach and discussed some of the various optimizations that are possible. Next to the

adaptively optimized choice of temperature steps that is by now well established [13, 22], it is also possible to choose the sweep protocol adaptively [23], or use PA for density-of-states estimation [24]. Here we focused on the freedoms involved in choosing a protocol for the resampling step as well as the possibilities inherent in the combination of individual runs through weighted averaging. For the former we find clear advantages for using nearest-integer resampling for the case of simulations with fluctuating population size and systematic resampling for fixed-size populations. Through providing minimal sampling variance, they lead to the least introduction of additional noise and correlation into the populations and hence result in smaller systematic and statistical errors as compared to other methods. Weighted averages provide the unique opportunity to reduce statistical *and* systematic errors through additional moderate-scale runs. Weighted averages can be shown rigorously to converge to the target (equilibrium) distribution. These as well as further, yet to be discovered, extensions of population annealing turn it into a possible candidate for a Swiss Army knife of computer simulations that should be one of the first methods of choice for practitioners in the field.

## References

1. Hukushima, K., Iba, Y.: Population annealing and its application to a spin glass. *AIP Conf. Proc.* **690**, 200–206 (2003)
2. Iba, Y.: Population Monte Carlo algorithms. *Trans. Jpn. Soc. Artif. Intell.* **16**, 279–286 (2001)
3. Machta, J.: Population annealing with weighted averages: A Monte Carlo method for rough free-energy landscapes. *Phys. Rev. E* **82**, 026704 (2010)
4. Weigel, M., Barash, L.Y., Shchur, L.N., Janke, W.: Understanding population annealing Monte Carlo simulations. *Phys. Rev. E* **103**, 053301 (2021).
5. Christiansen, H., Weigel, M., Janke, W.: Accelerating molecular dynamics simulations with population annealing. *Phys. Rev. Lett.* **122**, 060602 (2019)
6. Barash, L.Y., Weigel, M., Shchur, L.N., Janke, W.: Exploring first-order phase transitions with population annealing. *Eur. Phys. J. Spec. Top.* **226**, 595–604 (2017)
7. Rose, N., Machta, J.: Equilibrium microcanonical annealing for first-order phase transitions. *Phys. Rev. E* **100**, 063304 (2019)
8. Suruzhon, M., Bodnarchuk, M.S., Ciancetta, A., Wall, I.D., Essex, J.W.: Enhancing ligand and protein sampling using sequential Monte Carlo. *J. Chem. Theory Comput.* **18**, 3894–3910 (2022)
9. Geyer, C.J.: Markov chain Monte Carlo maximum likelihood. In: *Computing Science and Statistics: Proceedings of the 23rd Symposium on the Interface*, pp. 156–163. American Statistical Association, New York (1991)
10. Hukushima, K., Nemoto, K.: Exchange Monte Carlo method and application to spin glass simulations. *J. Phys. Soc. Jpn.* **65**, 1604–1608 (1996)
11. Sugita, Y., Okamoto, Y.: Replica-exchange molecular dynamics method for protein folding. *Chem. Phys. Lett.* **314**, 141–151 (1999)
12. Weigel, M.: Monte Carlo methods for massively parallel computers. In: Y. Holovatch (ed.) *Order, Disorder and Criticality*, vol. 5, pp. 271–340. World Scientific, Singapore (2018)

13. Barash, L.Y., Weigel, M., Borovský, M., Janke, W., Shchur, L.N.: GPU accelerated population annealing algorithm. *Comput. Phys. Commun.* **220**, 341–350 (2017)
14. Doucet, A., de Freitas, N., Gordon, N. (eds.): *Sequential Monte Carlo Methods in Practice*. Springer, New York (2001)
15. Wang, W., Machta, J., Katzgraber, H.G.: Population annealing: Theory and application in spin glasses. *Phys. Rev. E* **92**, 063307 (2015)
16. Moral, P.D., Doucet, A., Jasra, A.: On adaptive resampling strategies for sequential Monte Carlo methods. *Bernoulli* **18**, 252–278 (2012)
17. Gessert, D., Weigel, M., Janke, W.: Resampling schemes in population annealing – numerical results. *J. Phys.: Conf. Ser.* **2207**, 012012 (2022)
18. Gessert, D., Janke, W., Weigel, M.: Resampling schemes in population annealing – numerical and theoretical results. Preprint arXiv:2305.19994 (2023)
19. Ebert, P.L., Gessert, D., Weigel, M.: Weighted averages in population annealing: analysis and general framework. *Phys. Rev. E* **106**, 045303 (2022)
20. Janke, W. (ed.): *Rugged Free Energy Landscapes — Common Computational Approaches to Spin Glasses, Structural Glasses and Biological Macromolecules*, *Lect. Notes Phys.*, vol. 736. Springer, Berlin (2007)
21. Albash, T., Barash, L.N., Hen, I., Weigel, M.: Population annealing quantum Monte Carlo (2023). In preparation
22. Christiansen, H., Weigel, M., Janke, W.: Population annealing molecular dynamics with adaptive temperature steps. *J. Phys.: Conf. Ser.* **1163**, 012074 (2019)
23. Gessert, D., Janke, W., Weigel, M.: In preparation
24. Barash, L., Marshall, J., Weigel, M., Hen, I.: Estimating the density of states of frustrated spin systems. *New. J. Phys.* **21**, 073065 (2019)